Pergamon

Cement and Concrete Research 30 (2000) 1853–1860

CEMENT AND CONCRETE RESEARCH

# Fractal nucleation and growth model for the hydration of tricalcium silicate

Richard A. Livingston*

*Office of Infrastructure R&D, Federal Highway Administration, 6300 Georgetown Pike, McLean, VA 22101, USA*

Received 14 August 2000; accepted 19 October 2000

**Abstract**

The phase transformation kinetics of the tricalcium silicate reaction for the period of peak hydration rate can be described as a four-parameter exponential nucleation and growth model. The exponent in the model can take a noninteger value that may be an irrational number. Application of a fractal impingement model based on a mean field diffusion-limited aggregation (DLA) process results in a fractal nucleation and growth model. This indicates consistency between small-angle neutron scattering (microstructural) and quasi-elastic neutron scattering (kinetics) measurements. Also, the fractal basis of the exponent in the kinetics model precludes the interpretation of conventional grain growth processes. Concerning the analysis of kinetics data, the four-parameter form of the kinetics model means that the double logarithmic least squares fit to the kinetics data is not appropriate. Instead, a nonlinear curve fitting approach is necessary. © 2001 Elsevier Science Ltd. All rights reserved.

*Keywords:* Hydration; Microstructure; Fractal dimensions; $Ca_3SiO_5$; Modeling; Avrami equation; Diffusion-limited aggregation; Neutron scattering

## 1. Introduction

A fundamental aspect of materials science is the relationship between the microstructure and the chemical and physical reactions that produce it. Typically, a material does not uniformly and instantaneously arise from its precursors. Instead, the transformed phase grows from a collection of nucleation sites. The observed grain-size distribution is a function of the rate of reaction. This field is usually referred to as phase transformation kinetics. Much of the early work on phase transformation kinetics concerned metallurgical processes, either the solidification from melts or the transformation from one solid phase to another [1].

The volume fraction of the transformed phase, $X$, is found to be an exponential function of time, $t$:

$$X = \frac{V}{V_o} = 1 - \exp\{-[k(t - t_i)]^n\} \tag{1}$$

where $t_i$ is an induction time, $k$ is a rate constant, and $n$ is an exponent that characterizes the process. This equation is often, but somewhat inappropriately, called the Avrami equation. Here it will simply be referred to as the three-parameter ($k$, $t_i$, $n$) equation.

Several research groups listed in Table 1 have applied this model to tricalcium hydration kinetics, also including the interpretation of the exponent to characterize the physical processes involved. This approach assumes that the solid polycrystalline grain growth model developed for metals can be applied without modification to the development of the amorphous C-S-H gel. The objective of this paper is to propose an alternative model based on fractals, which is more consistent with the current state of knowledge of hydrated Portland cement microstructures.

## 2. Derivation of the phase transformation kinetics model

The derivation of the conventional three-parameter equation requires several mathematical models. One is the nucleation model, which describes the distribution in space and time of the sites where the transformed phase nucleates. The simplest form of the nucleation model assumes a uniform distribution of sites throughout the volume, and all sites are present instantaneously at $t = 0$. This is known as

---

* Tel.:+1-202-493-3063; fax:+1-202-493-3161.

*E-mail address*: dick.livingston@fhwa.dot.gov (R.A. Livingston).

PII: S0008-8846(00)00457-9

Table 1
Applications of the three-parameter kinetic model to $C_3S$ hydration data

| Method | Variable | Reference |
|---|---|---|
| X-ray diffraction | $C_3S$, CH volume fractions | Brown et al. [11] |
| Small-angle X-ray scattering | C-S-H surface area | Vollet and Craievich [29] |
| Raman scattering | $C_3S$, CH volume fractions | Tarrida et al. [30] |
| Quasi-elastic neutron scattering | Free- and boundwater volume fractions | Berliner et al. [13] |

the site-saturated, or instantaneous, nucleation model. It is often necessary to introduce an induction time, $t_i$, prior to the appearance of the initial nucleation sites, so that kinetics models are usually given in terms of $t - t_i$ as indicated in Eq. (1). In more sophisticated nucleation models, additional sites are allowed to form at $t > t_i$. This is referred to as continuous nucleation. Other nucleation models deviate from a uniform spatial distribution, such as allowing nucleation only on grain boundaries.

Having specified the nucleation model, the second necessary model describes how each site grows with time. These growth models are usually of the linear form $r \propto at$ where $r$ is the characteristic radius of the cluster or grain. For convenience, $a$ is usually assumed to be a constant with respect to time. However, in many cases, this rate constant is a function of temperature, typically following an Arrhenius-type behavior [Eq. (2)]:

$$k = k_o \exp\left(-\frac{E_a}{RT}\right) \tag{2}$$

where $E_a$ is the apparent activation energy and $R$ is the universal gas constant [2]. Consequently, $k$ is a constant only if the phase transformation takes place under isothermal conditions.

The third model is the impingement model, which describes how the individual growing grains interact with each other and inhibit further growth. This is illustrated in Fig. 1, which shows two growth sites separated by a distance $l$. In the case of continuous nucleation, both grow at the same rate, $a$, but one nucleates at $t = 0$ and the other at some later time, $\tau$. Then the time of impingement is:

$$t = \frac{1}{2}\left(\frac{l}{a} + \tau\right) \tag{3}$$

In the case of instantaneous nucleation, $\tau = 0$, and Eq. (3) collapses to $t = l/2a$.

Given these models, it is then possible to derive the three-parameter equation. This is often attributed to Avrami [3,4], but Johnson and Mehl [5] published a similar model almost simultaneously. However, in both cases, the derivation used a deterministic approach based on geometric arguments involving "phantom" nuclei and was incomplete. The first correct derivation, based on probabilistic arguments, may have been sketched out by Kolmogorov [6] in 1937. Consequently, the model is sometimes known as the Kolmogorov Avrami Johnson Mehl (KAJM) model. It will simply be called the three-parameter model here. This is still an area of active research, as shown, for example, by Van Siclen [7] and Yu [8].

A more accessible derivation of the model, based on probability theory, given by Chandrasekhar [9] is as follows: let the impingement probability $W(r) = w(r)\mathrm{d}r$ denote the probability that the nearest neighbor to a growing particle with its center at $r = 0$ occurs between $r$ and $r + \mathrm{d}r$. This is actually the joint probability that is the product of two conditions: (a) a particle actually exists in the spherical shell between $r$ and $r + \mathrm{d}r$, and b) the growing cluster has not already impinged at a distance $< r$, which is equivalent to the probability that no particle exists at a position $< r$. The probability distribution function for condition (a) is simply $4\pi r^2 N$, where $N$ is the number density of particles in the volume of interest. For condition (b) it should be noted that the probability of a particle not existing at a distance $< r$ is given by the complement of a particle occurring, or $1 - W(r)$. Then the probability density function $w(r)$ for the probability of impingement, $W(r)$, is [Eq. (4)]:

$$w(r) = 4\pi r^2 N\left[1 - \int_0^r w(r')\mathrm{d}r'\right] \tag{4}$$

where $r'$ is a variable of integration.

Going through the derivation presented in Appendix A eventually gives the result:

$$W(r) = 1 - \exp(-4\pi r^3 N/3) \tag{5}$$

The three-parameter phase transformation model, Eq. (1), can be recovered from Eq. (5) by noting that the result given

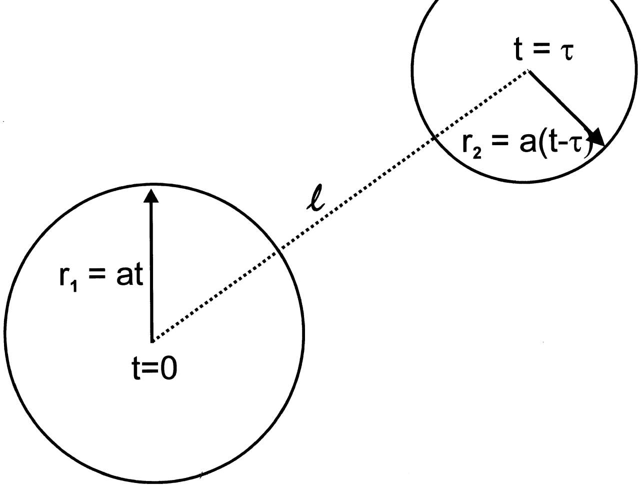

Fig. 1. Diagram of the impingement condition for between two growing grains, one nucleated at $t = 0$, the other at $t = \tau$.

by Eq. (A6) in Appendix A that the probability density function $w(r)$ is [Eq. (6)]:

$$w(r) = 4\pi r^2 N \exp(-4\pi r^3 N/3) \tag{6}$$

This impingement probability density function can also be interpreted as the probability of the nearest growing particle at $r$ [9]. Then the probability, $\psi$, that any given point in space is *not* contained within a growing particle is, according to Markworth [10] [Eq. (7)]:

$$\psi = \int_r^\infty w(r)\mathrm{d}r = \exp(-4\pi r^3 N/3) \tag{7}$$

Applying this probability to the total volume of interest yields the result that the volume fraction of unoccupied space is also $\psi$. Then the volume fraction of the growing phase is [Eq. (8)]:

$$X = 1 - \psi = 1 - \exp(-4\pi r^3 N/3) \tag{8}$$

Comparison with Eq. (1) and Fig. 1 shows that [Eq. (9)]:

$$a = k\,\sqrt[3]{3/4\pi N} \tag{9}$$

Both $a$ and $k$ are rate constants, but the former is defined in terms of a specific model of particle growth while the latter, which is typically obtained from experimental data, is defined in terms of the transformed volume fraction, $X$.

This derivation assumed a three-dimensional particle growth model and hence, $n = 3$. Derivations for one- or two-dimensional particle growth give similar results, and hence, the results can be generalized to $n$ dimensions.

The application of this three-parameter equation to data for phase transformation kinetics of metals involves measuring the volume fraction $X$ of the product phase at a series of times. Typically, this has been done by examining polished and etched samples under a metallographic microscope. The parameters $k$ and $n$ can then be found by linear regression on the transformed data [Eq. (10)]:

$$\ln[\ln(1 - X(t))] = n\ln(t) + n\ln(k) \tag{10}$$

This is known as the double logarithmic least squares fit. According to the original derivation, the exponent $n$ would have an integer value between 1 and 4. However, it was shown that $n$ could have a fractional, but rational, value depending on the type of growth process involved. This led to the concept that the value of the exponent could be interpreted to reveal the nature of phase transformation kinetics. This is summarized in the formula [11]:

$$n = (P/S + O) \tag{11}$$

where $P$ is the dimensionality for growth of product: $P = 1$, 2, or 3 for fibers, sheets, and polygons, respectively; $S = 1$ or 2 for interface or diffusion-controlled growth, respectively;

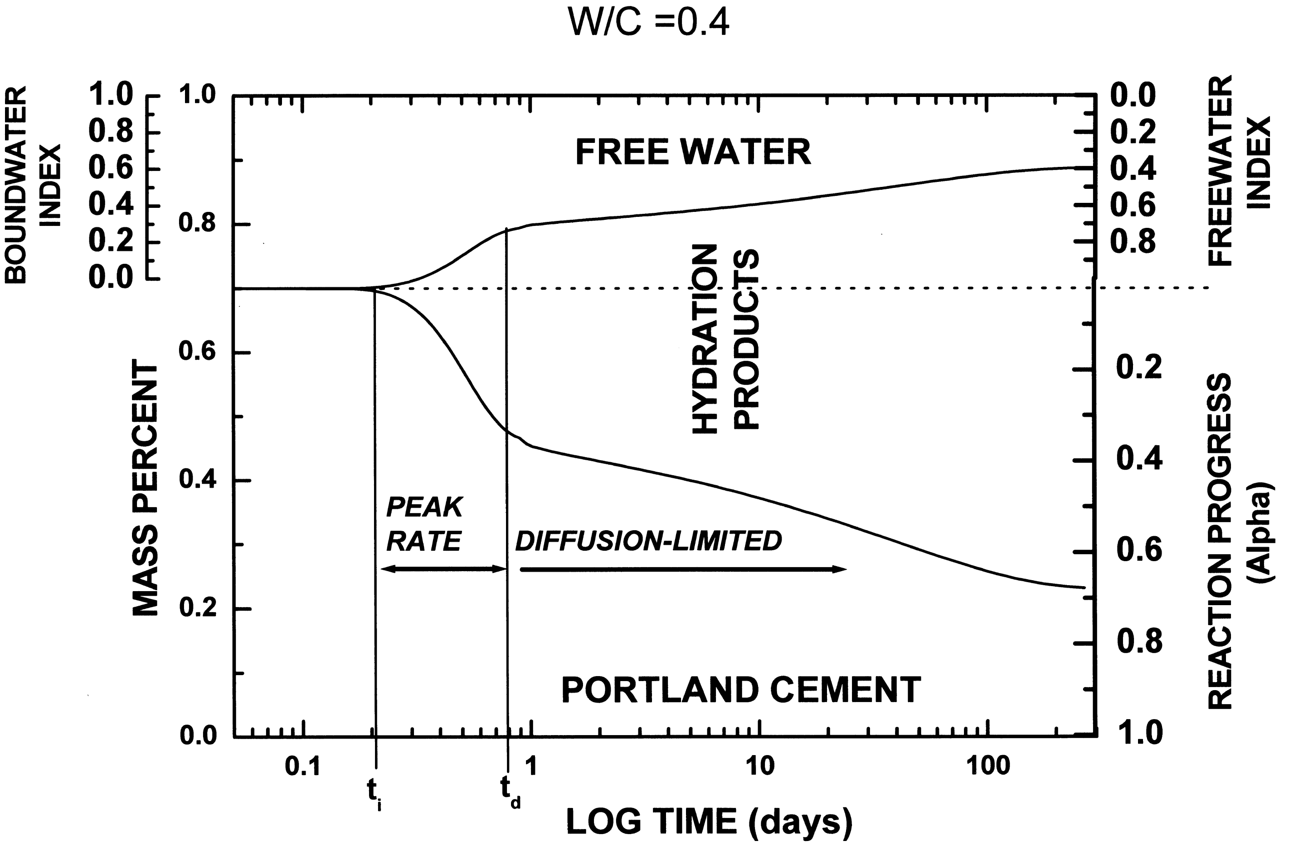

Fig. 2. Schematic diagram of the reaction progress of tricalcium silicate hydration, after Glasser et al. [28]. Peak reaction rate and diffusion-limited stages are indicated.

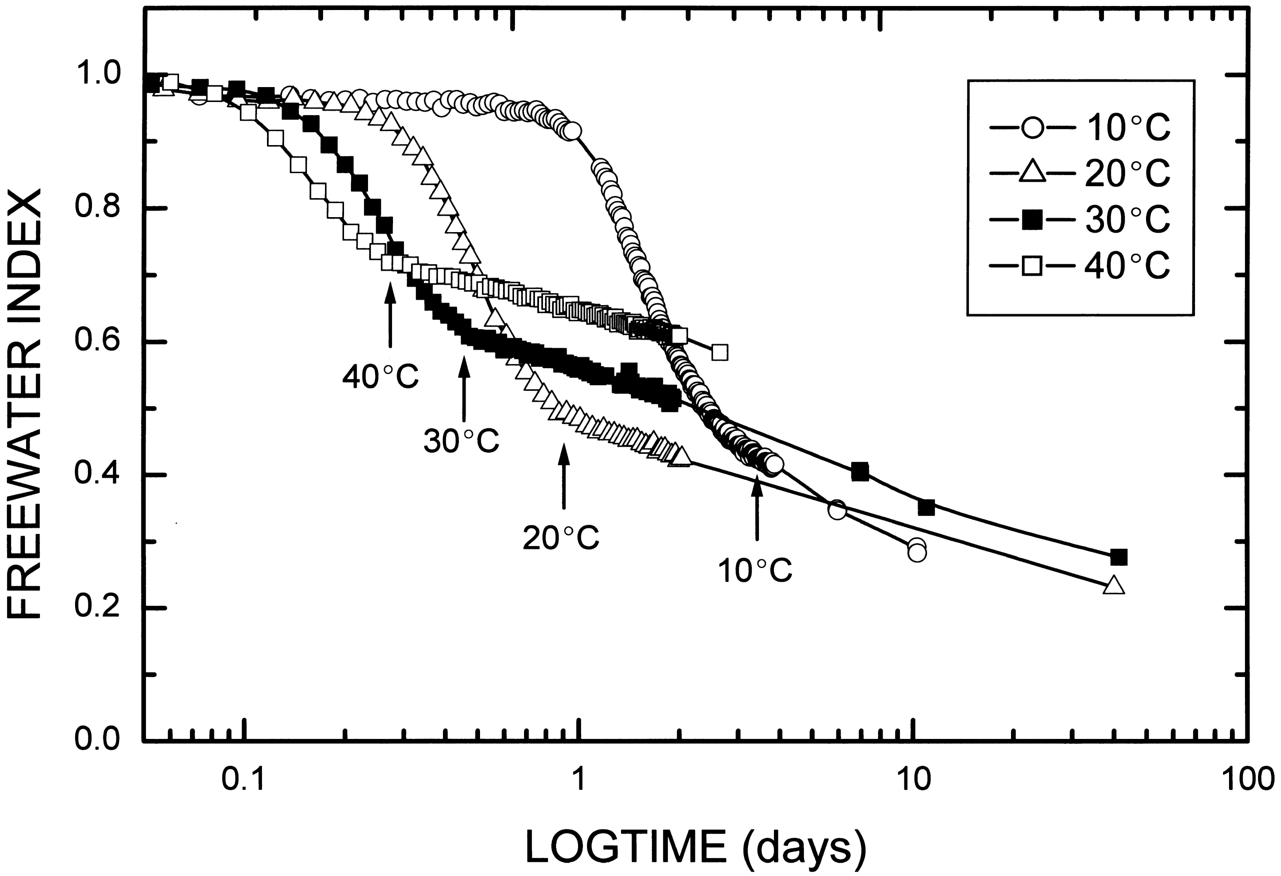

Fig. 3. Quasi-elastic neutron scattering data for isothermal hydration of tricalcium silicate fitted to four-parameter kinetics model [14]. Transitions from peak reaction rate to diffusion-limited stages are marked by arrows.

and $O = 0$ for site-saturated nucleation and 1 for continuous nucleation. Since all three factors are integers, $n$ is restricted to the set of rational numbers. However, as Christian [1] points out, this inversion process to infer growth mechanisms can yield ambiguous results.

## 3. Application of the three-parameter equation to tricalcium silicate hydration

In the investigation of the hydration kinetics of Portland cement, tricalcium silicate is often used as a simplified model system. This avoids the complexities introduced by the presence of other phases such as dicalcium silicate, while retaining the main reactant in Portland cement. The kinetics of the reaction is illustrated in Fig. 2, which plots the reaction progress variables as a function of time. Several stages can be identified [12]. The stage of interest for the phase transformation kinetics is the peak reaction stage, which begins at the end of the induction period, $t_i$, and ends at the beginning of the diffusion-limited stage, $t_d$.

The investigators listed in Table 1 extracted the parameters using the double logarithmic least square fit approach, but in each case, found that the exponent was considerably lower than would be expected. Nevertheless, Brown et al. [11] and Berliner et al. [13] proceeded to interpret the exponent using the relationship given by Eq. (11) to infer surface-type processes.

More recently FitzGerald et al. [14], applied quasi-elastic neutron scattering to obtain hydration kinetic data with a time resolution of 30 min [9]. As shown in Fig. 3, the data can be fitted using a four-parameter equation:

$$\mathrm{BWI}(t) - \mathrm{BWI}(t_i) = A\{1 - \exp[-\{k(t - t_i)\}^n]\} \tag{12}$$

where BWI is the boundwater index, the upper branch of the reaction curve in Fig. 2. FitzGerald et al. [14] presented a version of Eq. (12) terms of the freewater index, FWI, which is simply 1 − BWI, as shown in Fig. 2. The fourth parameter in this equation, the leading coefficient $A$, represents the asymptotic value of the amount of boundwater that can be formed as $t \rightarrow \infty$.

Pade and Struble [15] have referred to models of the form of Eq. (12) as "topochemical" after Yeremin [16] in the context of expansion test data. However, Cussler [17] and others have reserved this term for the specific case of diffusion through a surface layer followed by a chemical reaction, which gives kinetics that typically involve the square root of time. This type of time dependence in the hydration of $C_3S$ actually occurs after the period of peak nucleation and growth. Therefore, to avoid confusion, Eq. (12) will simply be called the four-parameter model.

It is evident that if $A \neq 1$, then the double logarithmic least squares linear regression cannot be applied to find the three parameters. The physical factors that determine $A$ for $C_3S$ hydration are still being investigated, but since the peak hydration rate stage only accounts for a fraction of volume the original phases present (Fig. 2), it is reasonable to assume that $A < 1$. The fact that Berliner et al. [13] and the other groups listed in Table 1 applied the double logarithmic least squares fit in this situation may explain why they obtained values for $n$ that differ so much from what would be expected. In contrast, FitzGerald et al. [14], using Eq. (12), found that $2 < n < 2.6$, which is consistent with nucleation and growth occurring in a three-dimensional pore space.

Thus, having obtained physically realistic values for $n$, the next question is whether these can interpreted to give insight into the nature of the process using Eq. (11). However, the experimental results do not yield integer values, or even rational numbers, for $n$. This may simply be due to uncertainties in the data and in the nonlinear curve fitting process. On the other hand, this raises the possibility that fractal dimensions may be involved. Given the known features of C-S-H microstructure, as reviewed below, this possibility must be given serious consideration.

## 4. Fractal microstructure of C-S-H gel

A number of researchers [18–20] have shown that the hydrated Portland cement paste has a fractal microstructure on the length scale of 1–1000 nm. The concept of fractals concerns objects that have dimensions that are not integers. The definitions of fractals and nomenclature in the literature are not completely consistent and can vary to a certain extent depending on the method of measuring the material [21]. In this case, the methods used on Portland cement paste have been small-angle X-ray [20] and neutron scattering [18]. These techniques yield directly the pair correlation function of the material, which relates the density function of the material at point $r_o$ with the density at some other position $r_o + r$. This density function is binary-valued, i.e. $\rho(r_o) = 1$ if the material is present at position $r_o$, and $\rho(r_o) = 0$ if it is absent. Then the pair correlation function has the form [22] [Eq. (13)]:

$$C(r) = \langle\langle \rho(r_o)\rho(r_o + r)\rangle\rangle_{|r|=r} \tag{13}$$

where $\langle\langle \ldots \rangle\rangle$ indicates averaging over all possible origins $r_o$ and all orientations. If the material is perfectly solid, then $C(r) = 1$. Otherwise, for example, in a porous solid, $C(r) < 1$.

The connection between the pair correlation function and fractals lies in the principle of self-similarity. That is, the fractal object has the same dimensional attributes independent of the length scale used to quantify it. This implies that the pair correlation function is homogeneous, i.e. [Eq. (14)]:

$$C(\lambda r) = \lambda^{\alpha} C(r) \tag{14}$$

where $\lambda$ is simply a scale factor that can vary over several orders of magnitude, and $\alpha$ is the fractal co-dimension defined as [Eq. (15)]:

$$\alpha \equiv d - D \tag{15}$$

where $d$ is the Euclidean dimension ($d = 1$ for a line, 2 for a surface, and 3 for a solid), and $D$ is the actual fractal dimensionality. If $2 < D < 3$ then the object is interpreted as a fractal volume. This can apply to porous materials over certain length scales. For $1 < D < 2$, the object can be interpreted as a fractal surface such as a sheet punctured by a set of holes of different sizes, also known as a gasket. However, there is another type of fractal surface, which is continuous but rough, like sandpaper in which the heights of the asperities has a fractal distribution. In this case, $D > 2$, but does not approach 3.

Although in theory a fractal structure can exist over many length scales, in most actual systems the fractal range is limited to few orders of magnitude of length. This is dealt with by introducing a characteristic correlation length, $\xi$, which defines the upper limit of the range by modifying the pair correlation function such that [23] [Eq. (16)]:

$$C(r) \sim rR^{\alpha} \exp(-r/\xi) \tag{16}$$

The lower limit, or cutoff, of the length range is set by the characteristic particle size, and it is usually symbolized by $r_c$.

Both fractal volumes and surfaces can be found in small-angle scattering studies of C-S-H as shown in Fig. 4. This is an idealized logarithmic plot of the data in the coordinates usually used in small-angle scattering. The vertical axis is

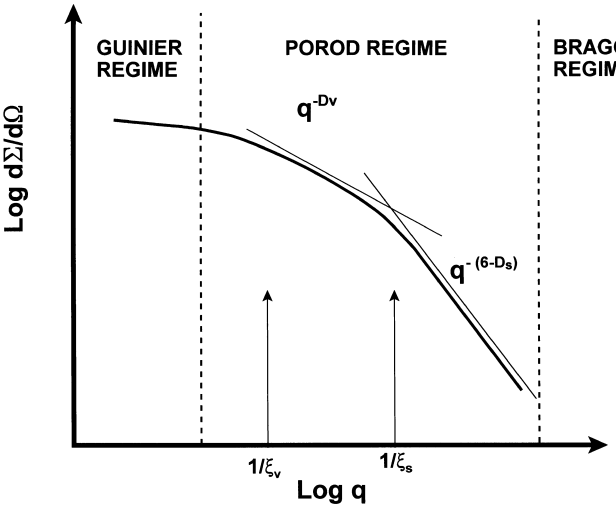

Fig. 4. Idealized small-angle scattering curve showing fractal features, after Kriechbaum et al. [19].

the macroscopic scattering cross-section, which is directly related to the pair correlation function. The horizontal axis is the scattering vector ***q***, which is the inverse of the length scale. In the region marked as the Porod scattering regime, the part to the right of the correlation length, $\xi_s$, is related to the amount of the C-S-H gel. From the slope of the curve, the fractal dimension of this surface, $D_s$, can be extracted, which has values in the range of 2.5–2.8 [24]. The part of the curve to the left of $\xi_s$ has a different slope, yielding a fractal dimension $D_v = 2.3$, and this interpreted as the rough surface of the reacting $C_3S$ grains.

Therefore, given the fractal nature of the microstructure and the apparent fractal exponent of the kinetics model, it is reasonable to inquire whether the hydration of Portland cement paste can be described in terms of a fractal nucleation and growth model.

## 5. Diffusion-limited aggregation

The origin of the fractal microstructure of gels such as C-S-H has been postulated to be the process of aggregation of individual colloidal particles into extended clusters. This process, referred to as diffusion-limited aggregation (DLA), has been investigated extensively with computer simulations. Fig. 5 illustrates the result of such a simulation. At each increment of time, a single colloidal particle is introduced at effectively the maximum distance from the growing cluster. It follows a random walk through the space until it encounters the cluster and then becomes attached. The compactness of the cluster depends on several parameters such as the sticking probability and whether the particle attaches invariably to the first point of the cluster it encounters.

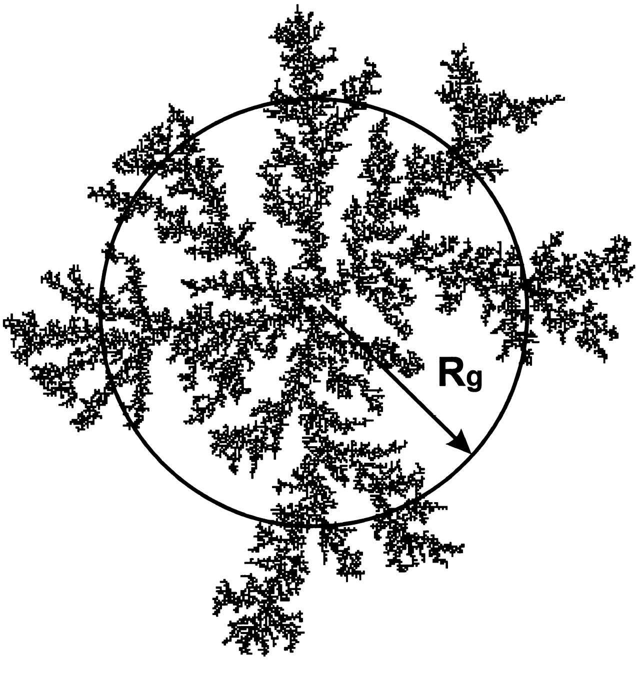

Fig. 5. Numerical simulation of the DLA cluster after an arbitrary number of cycles. The radius of gyration, $R_g$, is also shown.

Various properties of the DLA cluster have fractal aspects. Specifically, the radius of gyration of the cluster, $R_g$, is the density-weighted mean radius, as illustrated in Fig. 5. Numerical simulations have implied that this is related to the size of cluster, $s$, according to [22]:

$$s \sim R_g^D \tag{17}$$

where $D = 1.715 \pm 0.004$ for $d = 2$, and $2.49 \pm 0.01$ for $d = 3$. It should be noted that the size, $s$, is measured as the total number of particles making up the cluster.

Meakin and Deutch [25] have pointed out that in the specific case of cluster growth in a suspension of colloidal particles, the density of the outermost part of the cluster must asymptotically approach that of the suspension. Beyond this point, cluster growth is not fractal, but regular two- or three-dimensional. This limited range of fractal growth is set by introducing an appropriate correlation length factor, $\xi$.

## 6. Derivation of phase transformation kinetics using fractal impingement

As discussed above, there are three models that must be specified for the phase transformation process: nucleation, growth rate, and impingement. For the continuous nucleation process, probability theory leads to the conclusion that the time dependence would show a Poisson relationship rather than a fractal one [6].

The next requirement is the growth model. For DLA clusters, the essential growth relationship is between the size and the radius of gyration, Eq. (17). This has no explicit time dependence. Consequently, it is possible to introduce an arbitrary fractal time relationship for either $s$ or $R_g$, which can be shown to produce a fractal exponent. However, for simplicity, we assume, as in the conventional Euclidean space derivation, that the radius of gyration is a linear function of time, i.e. $R_g \propto at$.

This leaves the third possibility, a fractal equivalent of the impingement model. This involves a factor that consists of the locus of the nearest neighbors to the growing cluster, condition (a) above. In the case of the conventional theory, this becomes a spherical shell of radius $r$. In contrast, for the DLA cluster, Fig. 5 shows that the locus of outermost points, defined as the hull, is a spiky or rough surface. Unfortunately, there is no general analytic description for the hull, and consequently, case-specific numerical simulations have to be used [22].

As an approximation to the hull of the cluster, a sphere of radius $R_g$ is used. The volume of the DLA cluster can be found from its size, $s$, the total number of particles, and the characteristic volume of the individual colloidal particles, $v$. Hence, from Eq. (17) [Eq. (18)]:

$$V = vs \sim vR_{\mathrm{g}}^{D} \tag{18}$$

In Euclidean dimensions, the surface area of a sphere is the derivative of the volume with respect to the radius. Applying this concept to a fractal volume, we define a surface, $S$, such that:

$$S = \frac{\mathrm{d}V}{\mathrm{d}r} = 4\pi vDR_{\mathrm{g}}^{D-1} \tag{19}$$

Since $2<D<3$, the dimensionality of this surface is less than 2. This implies a smooth spherical surface with holes in it, somewhat like a wiffle ball.

Then the probability density function of impingement, $w(r)$, can be written, using the derivation of Section 2 [Eq. (20)]:

$$w(r) = 4\pi vDR_{\mathrm{g}}^{D-1}N\left[1 - \int_{0}^{R_{\mathrm{g}}} w(r')\mathrm{d}r'\right] \tag{20}$$

which, upon going through the steps in Appendix A, and substituting $R_{\mathrm{g}} \propto at$, gives [Eq. (21)]:

$$W(t) = 1 - \exp\{-4\pi vN(at)^{D}\} \tag{21}$$

Comparison with Eq. (12) shows that the exponent $n$ can thus be equated with the fractal dimensionality $D$. Therefore, the spatial fractal model of microstructure development leads to a fractal time model of the reaction kinetics. This implies that the agreement between the spatial fractal dimensionality of $\sim 2.5$ for the C-S-H gel measured by small-angle neutron scattering and the exponent of 2.5 found for the reaction kinetics measured by quasi-elastic neutron scattering is not simply fortuitous.

## 7. Discussion

The crucial step in the derivation of this fractal model of phase transformation kinetics is the assumption embodied in Eq. (19) that the impingement surface can be represented as the first derivative with respect to the radius of gyration of the size of the cluster. This results in a surface fractal dimensionality of $D-1$, which in this case is less than two, leading to the wiffle ball type surface. However, the actual hull would have $D>2$. This disagreement is a result of characterizing the cluster by the radius of gyration, which is the mean radius [26]. Consequently, the impingement surface model derived from this radius is a mean field approximation. Nevertheless, Eq. (19) can be justified on the basis that the actual surface of the cluster must be a function of its size, hence the derivative $\mathrm{d}V/\mathrm{d}S$ must exist, and by the chain rule, $\mathrm{d}V/\mathrm{d}r$ must also exist. This does not ensure that the derivative is a fractal itself, but it is difficult to conceive of a process by which a fractal volume generates a nonfractal hull. Computer simulations would be required to clarify this relationship.

It should be noted that the $D-1$ exponent of the surface results from applying the differential operator $\mathrm{d}^{n}/\mathrm{d}x^{n}$ with $n=1$ to the function $R_{\mathrm{g}}^{D}$. This is an unavoidable consequence of conventional calculus. However, it is not necessary to restrict the order of the operator to integer values of $n$. In fractional calculus it becomes possible to work with differential operators of the form $\mathrm{d}^{v}/\mathrm{d}x^{v}$ where $v$ can take on any value in the complex plane [27]. Thus, by defining the impingement surface as the appropriate fractional derivative of the cluster size, it would be possible to arrive at fractal dimensions of $D-v>2$.

Moreover, fractional calculus makes extensive use of the gamma function [Eq. (22)]:

$$\Gamma(v) = \int_{0}^{\infty} u^{v-1}e^{u}\mathrm{d}u \tag{22}$$

It can be seen that the probability of impingement defined in Eq. (A7) is a special case ($v=1$) of the incomplete gamma function [Eq. (23)]:

$$\gamma(v,x) = \frac{1}{\Gamma(v)}\int_{0}^{x} u^{v-1}e^{-u}du \tag{23}$$

This leads to the possibility that for phase transformation kinetics of fractal materials, it may be more appropriate to fit the data with an incomplete gamma function rather than with the three- or four-parameter exponential model. However, a detailed discussion of this issue is beyond the scope of this paper.

## 8. Conclusions

The phase transformation kinetics of the tricalcium silicate reaction during the peak hydration rate period can be described as a four-parameter exponential nucleation and growth model. However, the exponent in the model can be an irrational number reflecting a fractal process such as diffusion-limited aggregation. Also, the fractal basis of the exponent in the kinetics model precludes the interpretation of conventional grain growth processes. Concerning the analysis of kinetics data, the four-parameter form of the kinetics model means that the double logarithmic least squares fit to the kinetics data is not appropriate. Instead, a nonlinear curve fitting approach is necessary.

Applying a fractal model of cluster growth based on diffusion-limited aggregation leads to a fractal time model of the reaction kinetics. This implies that the agreement between the spatial fractal dimensionality of $\sim 2.5$ for the C-S-H gel measured by small-angle neutron scattering, and exponent of 2.5 found for the reaction kinetics measured by quasi-elastic neutron scattering is not simply fortuitous.

## Acknowledgments

The author would like to thank A. Allen for many helpful discussions and M. Oskard for a painstaking review of the mathematics.

## Appendix A.

Given the probability density function for impingement:

$$w(r) = 4\pi r^2 N\left[1 - \int_0^r w(r')\mathrm{d}r'\right] \tag{A1}$$

differentiating:

$$\frac{\mathrm{d}w(r)}{\mathrm{d}r} = 8\pi rN\left[1 - \int_0^r w(r')\mathrm{d}r'\right] - 4\pi r^2 Nw(r) \tag{A2}$$

or, substituting Eq. (A1) into Eq. (A2), we have [Eq. (A3)]:

$$\frac{\mathrm{d}w(r)}{\mathrm{d}r} = \frac{2w(r)}{r} - 4\pi r^2 Nw(r) \tag{A3}$$

Dividing through by $4\pi r^2 N$ and rearranging gives [Eq. (A4)]:

$$\frac{\mathrm{d}w(r)}{4\pi r^2 N\mathrm{d}r} - \frac{w(r)}{2\pi r^3 N} = -w(r) \tag{A4}$$

which, as Chandresekhar [9] has pointed out, can be rewritten as [Eq. (A5)]:

$$\frac{\mathrm{d}}{\mathrm{d}r}\left[\frac{w(r)}{4\pi r^2 N}\right] = -4\pi r^2 N\frac{w(r)}{4\pi r^2 N} \tag{A5}$$

and this can be finally integrated to give:

$$w(r) = 4\pi r^2 N\exp(-4\pi r^3 N/3) \tag{A6}$$

This is the probability density function. Hence, the probability of impingement at $r' < r$ is:

$$\begin{aligned} W(r) &= \int_0^r 4\pi N r'^2 \exp(-4\pi r'^3 N/3)\mathrm{d}r' \\ &= 1 - \exp(-4\pi r^3 N/3) \end{aligned} \tag{A7}$$

## References

[1] J.W. Christian, The Theory of Transformations in Metals and Alloys, Pergamon, Oxford, 1975.

[2] K.J. Laidler, Chemical Kinetics, third ed., HarperCollins, New York, 1987.

[3] M. Avrami, Kinetics of phase change: I, J. Chem. Phys. 7 (1939) 1103–1112.

[4] M. Avrami, Kinetics of phase change: II. Transformation–time relations for random distribution of nuclei, J. Chem. Phys. 8 (1940) 212–224.

[5] W.A. Johnson, R.F. Mehl, Reaction kinetics in processes of nucleation and growth, Trans. AIME 135 (1939) 416 – 441.

[6] A.N. Kolmogorov, k' Statisticheskoi Teorii Kristallizatsii Metallov, Izv. Akad. Nayuk CCCR, 2 (1937) 355–359.

[7] C.D. Van Siclen, Random nucleation and growth kinetics, Phys. Rev. B 54 (17) (1996) 11845–11854.

[8] G. Yu, General equation of the kinetics of phase transformations with a nucleation-and-growth mechanism, Philos. Mag. Lett. 75 (1) (1997) 43–48.

[9] S. Chandrasekhar, Stochastic problems in physics, Rev. Mod. Phys. 15 (1943) 1–89.

[10] A.J. Markworth, Analysis of the extent of growth-induced impingement for a simple model of precipitate nucleation and growth, Scr. Metall. 18 (1984) 1309–1311.

[11] P.W. Brown, J. Pommersheim, G. Frohnsdorff, A kinetic model for the hydration of tricalcium silicate, Cem. Concr. Res. 15 (1985) 35–41.

[12] E.M. Gartner, J.M. Gaidis, Hydration mechanisms: I, in: J.P. Skalny (Ed.), Materials Science of Concrete I, American Ceramic Society, Westerville, OH, 1989, pp. 95–125.

[13] R. Berliner, M. Popovici, K.W. Herwig, M. Berliner, H.M. Jennings, J.J. Thomas, Quasi-elastic neutron scattering study of the effect of water-to-cement ratio on the hydration kinetics of tricalcium silicate, Cem. Concr. Res. 28 (2) (1998) 231–244.

[14] S. FitzGerald, D. Neumann, J. Rush, R. Livingston, In-situ quasi-elastic neutron scattering measurement of the hydration of tricalcium silicate, Chem. Mater. 10 (1) (1998) 397–402.

[15] C. Pade, L.J. Struble, Kinetics and microstructural changes associated with mortar expansion, Cem. Concr., Aggregates 22 (1) (2000) 55–62.

[16] E.N. Yeremin, The Foundations of Chemical Kinetics, MIR, Moscow, 1979.

[17] E.L. Cussler, Diffusion: Mass Transfer in Fluid Systems, Cambridge Univ. Press, Cambridge, 1984.

[18] A.J. Allen, R.C. Oberthur, D. Pearson, P. Schofield, C.R. Wilding, Development of the fine porosity and gel structure of hydrating cement systems, Philos. Mag. B 56 (3) (1987) 263–288.

[19] M. Kriechbaum, G. Degovics, P. Laggner, J. Tritthart, Investigations on cement pastes by small-angle X-ray scattering and BET: The relevance of fractal geometry, Adv. Cem. Res. 6 (23) (1994) 93–101.

[20] D. Winslow, J.M. Bukowski, J.F. Young, The fractal arrangement of hydrated cement paste, Cem. Concr. Res. 25 (1) (1995) 147–156.

[21] D. Stoyan, H. Stoyan, Fractals, Random Shapes and Point Fields: Methods of Geometrical Statistics, Wiley, New York, 1994.

[22] P. Meakin, Fractals, Scaling and Growth Far from Equilibrium, Cambridge Univ. Press, Cambridge, 1998.

[23] S.K. Sinha, Scattering from fractal structures, Physica D 38 (1989) 310–314.

[24] A.J. Allen, R.A. Livingston, Relationship between differences in silica fume additives and fine-scale microstructural evolution in cement-based materials, Adv. Cem. Based Mater. 8 (1998) 118–131.

[25] P. Meakin, J.M. Deutch, Monte Carlo simulation of diffusion controlled colloid growth rates in two and three dimensions, J. Chem. Phys. 80 (5) (1984) 1.

[26] D.W. Schaefer, K.D. Keefer, Fractal geometry of silica condensation polymers, Phys. Rev. Lett. 53 (14) (1984) 1383–1386.

[27] R. Gorenflo, F. Mainardi, Fractional calculus: Integral and differential equations of fractional order, in: A. Carpinteri, F. Mainardi (Eds.), Fractals and Fractional Calculus in Continuum Mechanics, Springer, New York, 1997, pp. 223–276.

[28] F. Glasser, S. Diamond, D. Roy, Hydration reactions in cement pastes incorporating fly ash and other pozzolanic materials, in: L.J. Struble, P.W. Brown (Eds.), Microstructural Development During Hydration of Cement, Materials Research Society, Pittsburgh, 1987, pp. 167–186.

[29] D.R. Vollet, A.F. Craievich, Structure and kinetics of formation of the gel phase in hydrated tricalcium silicate, 8th International Congress on the Chemistry of Cement, Abla Grafica e Editora, Rio de Janeiro, 1986, pp. 330–336.

[30] M. Tarrida, M. Madon, B.L. Rolland, P. Colombet, An in-situ Raman spectroscopy study of the hydration of tricalcium silicate, Adv. Cem. Based Mater. 2 (1995) 167.